Three-Operator Proximal Splitting Scheme for 3-D Seismic Data Reconstruction

Yufeng Wang, Hui Zhou, Shaohuan Zu, Weijian Mao, and Yangkang Chen

***Abstract*— The proximal splitting algorithm, which reduces complex convex optimization problems into a series of smaller subproblems and spreads the projection operator onto a convex set into the proximity operator of a convex function, has recently been introduced in the area of signal processing. Following the splitting framework, we propose a novel three-operator proximal splitting (TOPS) algorithm for 3-D seismic data reconstruction with both singular value decomposition (SVD)-based low-rank constraint and curvelet-domain sparsity constraint. Compared with the well-known forward–backward splitting (FBS) method, our proposed TOPS algorithm can be flexibly employed to recover a signal satisfying double convex constraints simultaneously, such as low-rank constraint and sparsity constraint used in this letter. We have used both synthetic and field data examples to demonstrate the superior performance of the TOPS method over traditional SVD-based low-rank method and curvelet-domain sparsity method based on the FBS framework.**

***Index Terms*— Convex optimization, low rank, sparsity, three-operator proximal splitting (TOPS).**

I. Introduction

With the development of nonlinear analysis in mathematics in the late 1950s, convex optimization has become increasingly prevalent for computing reliable solutions in a broad spectrum of applications [1], [2], which can be generally formulated as the following form:

$$\min_{x \in \mathbb{R}^N} \; f_1(x) + f_2(x) + \cdots + f_m(x) \tag{1}$$

where $f_1, f_2, \ldots, f_m$ are a series of convex functions. Conventional smooth optimization techniques, such as gradient-based methods, may fail to tackle this problem when some of the convex functions are not differentiable. Operator splitting schemes provide a feasible solution to overcome this limitation by splitting complex problems into a set of smaller subproblems that can be solved individually [3]–[6]. In the past decade, many large-scale applications in machine learning, signal processing, and imaging have stimulated a significantly increased interest in operator-splitting-based algorithms, such as forward–backward splitting (FBS) [3], [7], Douglas–Rachford splitting (DRS) [4], forward–backward–forward splitting [5], and their generalizations and enhancements, such as generalized FBS [8] and three-operator splitting (TOS) [6].

Projection onto convex sets, which is designed for synthesizing a signal satisfying simultaneously several convex constraints, has become one of the most widely used convex optimization splitting algorithms in digital signal processing [9], [10]. However, projection methods are not appropriate to tackle problem (1) with more general constraints. The proximity operator of a convex function is a natural extension of the notion of a projection operator onto a convex set [1], [7]. Based on operator splitting scheme, the proximal formalism provides a unifying framework for analyzing and developing a broad class of convex optimization algorithms, such as iterative shrinkage thresholding [11], [12] and alternating-direction method of multipliers [1].

In this letter, we propose a three-operator proximal splitting (TOPS) method for 3-D seismic data reconstruction, which is an indispensable precondition procedure to remove sampling artifacts and to obtain high-quality seismic data [13], [14]. In comparison with conventional two-operator-splitting-based algorithms (e.g., FBS and DRS) mentioned above, TOPS scheme proposed here is particularly well adapted for synthesizing a signal satisfying simultaneously double convex constraints. Motivated by the low-rank property of seismic signal and sparsity property of seismic signal in the sparse transform domain [15]–[17], we therefore propose the TOPS method with both singular value decomposition (SVD)-based low-rank constraint and curvelet-domain sparsity constraint for seismic data reconstruction. Unlike the recently proposed hybrid rank-sparsity constraint (HRSC) model [16], our proposed TOPS scheme is a mathematically convergent algorithm to handle optimization problem satisfying double convex constraints simultaneously, whereas HSRC is more likely a hybrid strategy, where rank reduction and sparsity-promoting transforms are two specific constrains. To further demonstrate the feasibility and superior performance of our proposed algorithm, we conduct 3-D seismic data recovery in the framework of TOPS with double constraints using both synthetic and field data examples. For comparison, the results obtained by conventional FBS with individual low-rank constraint and individual sparsity constraint are also provided.

Manuscript received May 23, 2017; revised July 19, 2017; accepted August 3, 2017. Date of publication August 29, 2017; date of current version September 25, 2017. This work was supported in part by the National Natural Science Foundation of China under Grant 41174119, in part by the 973 Program of China under Grant 2013CB228603, in part by the National Science and Technology Program under Grant 2016ZX05010001-002, and in part by the Major Project of the China National Petroleum Corporation under Grant 2016A-3304. *(Corresponding author: Hui Zhou.)*

Y. Wang, H. Zhou, and S. Zu are with the State Key Laboratory of Petroleum Resources and Prospecting, China University of Petroleum, Beijing 102200, China (e-mail: huizhou@cup.edu.cn).

W. Mao is with the Center for Computational and Exploration Geophysics, State Key Laboratory of Geodesy and Earth's Dynamics, Chinese Academy of Geosciences, Institute of Geodesy and Geophysics, Wuhan 430077, China.

Y. Chen is with the Oak Ridge National Laboratory, National Center for Computational Sciences, Oak Ridge, TN 37831 USA (e-mail: ykchen@utexas.edu).

Color versions of one or more of the figures in this letter are available online at http://ieeexplore.ieee.org.

Digital Object Identifier 10.1109/LGRS.2017.2737786

II. METHODS

In this section, we first briefly introduce the general seismic reconstruction problem in the viewpoint of convex optimization problem. We also investigate two classes of widely used convex constraints, namely, the low-rank and sparsity constraints. We discuss in detail the conventional FBS algorithms with single constraint and TOPS algorithm with double constraints.

A. Seismic Data Reconstruction

In many signal recovery problems such as image inpainting and interpolation, we record an observation $\mathbf{d}_{\text{obs}}$ of original data $\mathbf{d}$ degraded by a sampling matrix $\mathbf{S}$ and corrupted by noise. In the spirit of convex optimization problem, let us suppose that f_m in problem (1) is β-Lipschitz differentiable

$$f_m(\mathbf{d}) = \frac{1}{2} \parallel \mathbf{Sd} - \mathbf{d}_{\text{obs}} \parallel_2^2 \tag{2}$$

which leads to Lipschitz constant $\beta = \parallel \mathbf{S} \parallel^2$. Hence, the general seismic data reconstruction problem can be summarized as

$$\min_{\mathbf{d}\in\mathbb{R}^N} \sum_{i=1}^{m-1} f_i(\mathbf{d}) + \cdots + \frac{1}{2} \parallel \mathbf{Sd} - \mathbf{d}_{\text{obs}} \parallel_2^2 \tag{3}$$

where $(1/2) \parallel \mathbf{Sd} - \mathbf{d}_{\text{obs}} \parallel_2^2$ plays the role of a data fidelity term and f_i models *a priori* knowledge about $\mathbf{d}$, which can be both smooth and nonsmooth. Benefited from the operator-splitting scheme, each nonsmooth constraint function in (3) is involved via its proximity operator individually.

In this letter, we adopt both low-rank constraint and sparsity constraint to recover 3-D seismic data. More specifically, we pose low-rank constraint on seismic data by utilizing singular value thresholding with its proximity operator as

$$\mathbf{prox}_{\lambda f}(\mathbf{d}) = \mathbf{Udiag}(\mathbf{prox}_{\lambda f}(d))\mathbf{V}^T \tag{4}$$

where $\mathbf{d} = \mathbf{Udiag}(d)\mathbf{V}^T$ is the SVD of $\mathbf{d}$. $\mathbf{prox}_{\lambda f}$ is the proximity operator with an input parameter λ. **diag** denotes a diagonal matrix composed of the singular values after SVD. In addition to the low-rank constraint, we also conduct sparsity constraint by transforming seismic data into curvelet domain [18]. Thus, the proximity operator can be expressed as

$$\mathbf{prox}_{\lambda f}(\mathbf{d}) = \mathcal{C}^{-1}\mathbf{prox}_{\lambda f}(\mathcal{C}\mathbf{d}) \tag{5}$$

where $\mathcal{C}$ and $\mathcal{C}^{-1}$ denote a pair of forward and inverse curvelet transforms, respectively.

B. Forward–Backward Splitting Scheme

We consider two $(m = 2)$ functions in (3) with f_2 being β-Lipschitz differentiable. The solutions to this convex optimization can be characterized by the following iteration:

$$\mathbf{d}^{k+1} = \mathbf{prox}_{\lambda f_1}(\mathbf{d}^k - \lambda \nabla f_2(\mathbf{d}^k)) \tag{6}$$

where λ is a step-size parameter. This type of scheme is known as an FBS algorithm, which breaks up every iteration step into a forward gradient step using function f_2 and a backward proximal step using function f_1. This algorithm converges

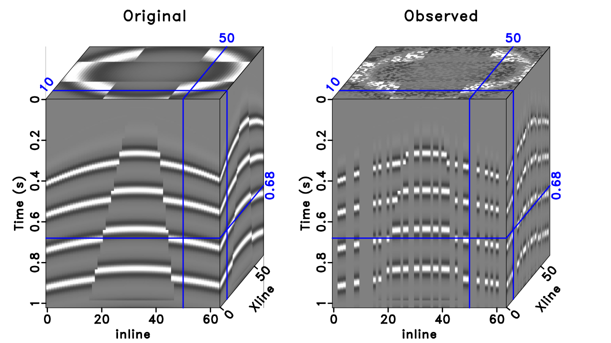

(a) (b)

Fig. 1. (a) Synthetic data. (b) Decimated synthetic data with 50% randomly removed traces.

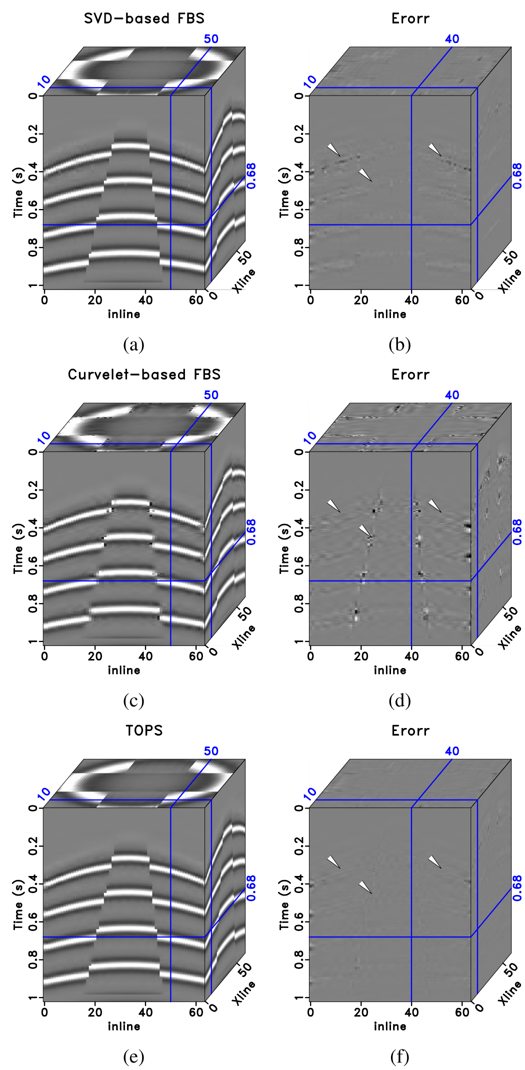

Fig. 2. Reconstructed synthetic data using (a) SVD-based FBS, (c) curvelet-based FBS, and (e) TOPS. The corresponding error of (b) SVD-based FBS, (d) curvelet-based FBS, and (f) our proposed TOPS scheme. Thresholding factor $\omega = 0.1$ for SVD-based FBS, $\omega = 0.05$ for curvelet-based FBS, and $\omega_1 = 0.05$ and $\omega_2 = 0.1$ for TOPS.

with rate $O(1/k)$ when f_2 is β-Lipschitz differentiable and step size $\lambda \in (0, 1/\beta]$. The convex function f_1 in (6) can be any convex constraint function that aims at promoting the

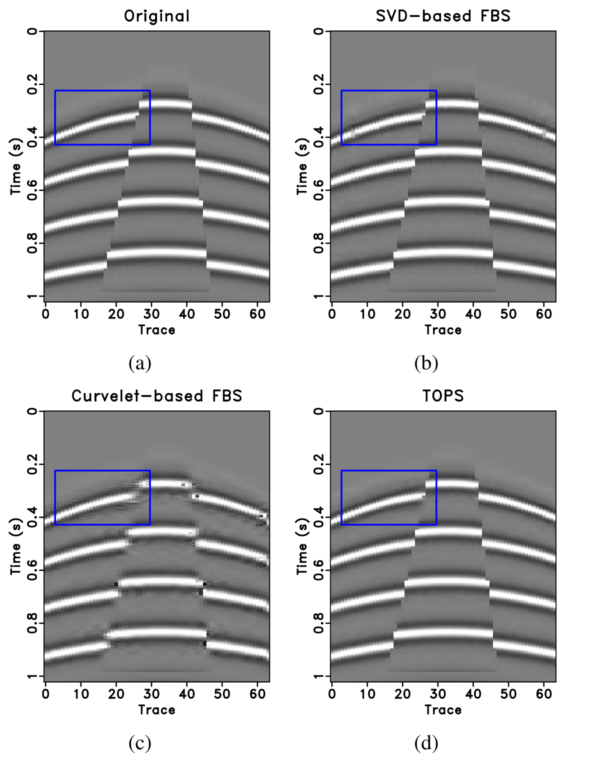

Fig. 3. Eighth crossline slice of (a) original data, and the reconstructed data using (b) SVD-based FBS, (c) curvelet-based FBS, and (d) our proposed TOPS scheme.

performance of signal recovery. Seismic data reconstruction problem in the framework of FBS with individual SVD-based low-rank constraint thus can be implemented in Algorithm 1.

Algorithm 1 SVD-Based FBS Algorithm

Input: Observed seismic data $\mathbf{d}_{\text{obs}}$; sampling matrix $\mathbf{S}$; step size parameter λ; thresholding factor ω; iteration number $niter$; fixed-point residual $\mathbf{r}_f$; tolerance for residual $\mathbf{r}_t$.
Output: Recovered seismic data $\mathbf{d}$.

Initialize: any initial $\mathbf{d}_0$;
for $k = 1 \cdots niter$ **do**
  $\mathbf{d}^{(k)} \leftarrow \mathbf{d}^{(k)} - \lambda \mathbf{S}(\mathbf{d}_{\text{obs}} - \mathbf{d}^{(k)})$;
  $\mathbf{d}^{(k)} \leftarrow \mathbf{U}\mathbf{diag}(\mathbf{prox}_{\lambda f}(\omega d^{(k)}))\mathbf{V}^T$;
  $\mathbf{r}_t^{(k)} \leftarrow \mathbf{norm}(\mathbf{d}_{\text{obs}} - \mathbf{d}^{(k)})/\mathbf{norm}(\mathbf{d}^{(k)})$;
  $\mathbf{r}_f^{(k)} \leftarrow \mathbf{norm}(\mathbf{d}^{(k)} - \mathbf{d}^{(k-1)})$;
  if $\mathbf{r}_f^{(k)} < \mathbf{r}_f \,||\, \mathbf{r}_t^{(k)} < \mathbf{r}_t$ **then**
    $break$;
  end if
end for

Algorithm 2 demonstrates the basic framework of curvelet-based sparsity constrained FBS algorithm.

C. Three-Operator Splitting Scheme

The TOS scheme was recently proposed in [6] to optimize composite objective functions with two possible nonsmooth convex functions for which we have access to their proximity operator. Here, we extend the case of $m = 2$ to $m = 3$ in

Algorithm 2 Curvelet-Based FBS Algorithm

Input: Observed seismic data $\mathbf{d}_{\text{obs}}$; sampling matrix $\mathbf{S}$; step size parameter λ; thresholding factor ω; iteration number $niter$; fixed-point residual $\mathbf{r}_f$; tolerance for residual $\mathbf{r}_t$.
Output: Recovered seismic data $\mathbf{d}$.

Initialize: any initial $\mathbf{d}_0$;
for $k = 1 \cdots niter$ **do**
  $\mathbf{d}^{(k)} \leftarrow \mathbf{d}^{(k)} - \lambda \mathbf{S}(\mathbf{d}_{\text{obs}} - \mathbf{d}^{(k)})$;
  $\mathbf{d}^{(k)} \leftarrow \mathcal{C}^{-1}\mathbf{prox}_{\lambda f}(\omega \mathcal{C}\mathbf{d}^{(k)})$;
  $\mathbf{r}_t^{(k)} \leftarrow \mathbf{norm}(\mathbf{d}_{\text{obs}} - \mathbf{d}^{(k)})/\mathbf{norm}(\mathbf{d}^{(k)})$;
  $\mathbf{r}_f^{(k)} \leftarrow \mathbf{norm}(\mathbf{d}^{(k)} - \mathbf{d}^{(k-1)})$;
  if $\mathbf{r}_f^{(k)} < \mathbf{r}_f \,||\, \mathbf{r}_t^{(k)} < \mathbf{r}_t$ **then**
    $break$;
  end if
end for

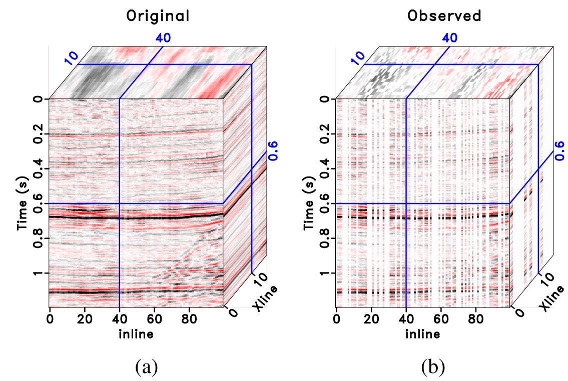

Fig. 4. (a) Field data. (b) Decimated field data with 50% randomly removed traces.

problem (1) and recall the convex optimization problem in the context of seismic data recovery

$$\min_{\mathbf{d}\in\mathbb{R}^N} \ \omega_1 f_1(\mathbf{d}) + \omega_2 f_2(\mathbf{d}) + \frac{1}{2} \parallel \mathbf{S}\mathbf{d} - \mathbf{d}_{\text{obs}} \parallel_2^2 \tag{7}$$

where ω_1 and ω_2 are penalty parameters. An averaging operator T is also provided to encode a solution to problem (7), i.e., solving the following fixed point equation [6]:

$$\mathbf{d}^{k+1} = (1 - \gamma_k)\mathbf{d}^k + \gamma_k T \mathbf{d}^k \tag{8}$$

where γ_k is a relaxation parameter and

$$T = I - \mathbf{prox}_{\lambda f_2} + \mathbf{prox}_{\lambda f_1} \circ (2\mathbf{prox}_{\lambda f_2} - I - \lambda \nabla f_3 \circ \mathbf{prox}_{\lambda f_2}) \tag{9}$$

where f_3 denotes the data fidelity term $(1/2) \parallel \mathbf{S}\mathbf{d} - \mathbf{d}_{\text{obs}} \parallel_2^2$; thus, (8) can be implemented as follows.

For $k = 0, 1, \ldots, niter$, do the following.

1) Get $\mathbf{d}_2^k = \mathbf{prox}_{\lambda f_2}(\mathbf{d}^k)$.
2) Get $\mathbf{d}_1^k = \mathbf{prox}_{\lambda f_1}\big(2\mathbf{d}_2^k - \mathbf{d}^k - \lambda \nabla f_3(\mathbf{d}_2^k)\big)$.
3) Get $\mathbf{d}^{k+1} = \mathbf{d}^k + \gamma_k\big(\mathbf{d}_1^k - \mathbf{d}_2^k\big)$.

In this letter, we combine TOS scheme with the essence of proximal algorithm, and further formulate a general TOPS framework containing both SVD-based low-rank constraint

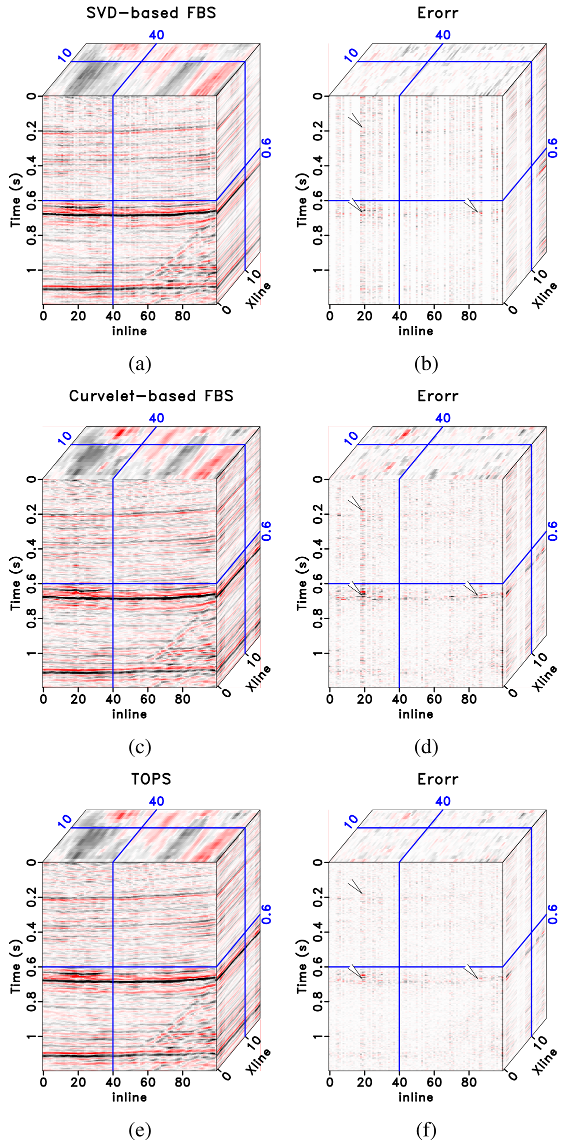

Fig. 5. Reconstructed field data using (a) SVD-based FBS, (c) curvelet-based FBS, and (e) TOPS. The corresponding error of (b) SVD-based FBS, (d) curvelet-based FBS, and (f) our proposed TOPS scheme. Thresholding factor $\omega = 1$ for SVD-based FBS, $\omega = 10$ for curvelet-based FBS, and $\omega_1 = 10$ and $\omega_2 = 1$ for TOPS.

and curvelet-domain sparsity constraint. Then the above seismic data recovery problem can be specifically represented as

$$\min_{\mathbf{d}\ \in \mathbb{R}^N} \omega_1 \parallel \mathcal{C}\mathbf{d} \parallel_1 + \omega_2 \parallel \mathbf{d} \parallel_* + \frac{1}{2} \parallel \mathbf{S}\mathbf{d} - \mathbf{d}_{\text{obs}} \parallel_2^2 . \quad (10)$$

The detailed algorithm workflow of the TOPS method with double convex constraints is shown in Algorithm 3.

Algorithm 3 Double-Constrained TOPS Algorithm

Input: Observed seismic data $\mathbf{d}_{\text{obs}}$; sampling matrix $\mathbf{S}$; step size parameter λ; penalty parameters ω_1 and ω_2; iteration number $niter$; fixed-point residual $\mathbf{r}_f$; tolerance for residual $\mathbf{r}_t$.

Output: Recovered seismic data $\mathbf{d}$.

Initialize: any initial $\mathbf{d}_0$;
for $k = 1 \cdots niter$ **do**
  $\mathbf{d}_2^{(k)} \leftarrow \mathbf{Udiag}(\mathbf{prox}_{\lambda f_2}(\omega_2\ d^{(k)}))\mathbf{V}^T$;
  $\mathbf{d}_1^{(k)} \leftarrow \mathcal{C}^{-1}\mathbf{prox}_{\lambda f_1}\{\omega_1 \mathcal{C}[2\mathbf{d}_2^{(k)} - \mathbf{d}^{(k)} - \lambda \mathbf{S}(\mathbf{d}_{\text{obs}} - \mathbf{d}_2^{(k)})]\}$;
  $\mathbf{d}^{(k)} \leftarrow \mathbf{d}^{(k)} + \gamma_k\ (\mathbf{d}_1^{(k)} - \mathbf{d}_2^{(k)})$;
  $\mathbf{r}_t^{(k)} \leftarrow \mathbf{norm}(\mathbf{d}_{\text{obs}} - \mathbf{d}^{(k)})/\mathbf{norm}(\mathbf{d}^{(k)})$;
  $\mathbf{r}_f^{(k)} \leftarrow \mathbf{norm}(\mathbf{d}^{(k)} - \mathbf{d}^{(k-1)})$;
  if $\mathbf{r}_f^{(k)} < \mathbf{r}_f \ || \ \mathbf{r}_t^{(k)} < \mathbf{r}_t$ **then**
    break;
  end if
end for

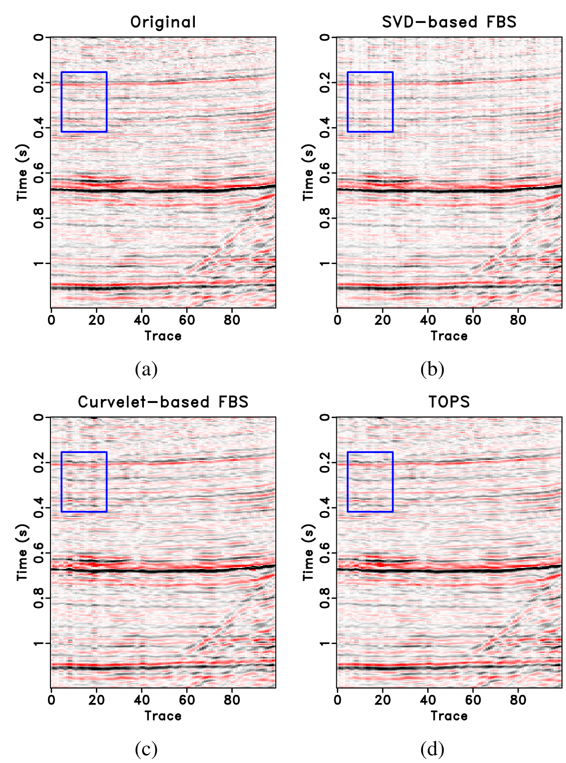

Fig. 6. Eighth crossline slice of (a) original data and the reconstructed data using (b) SVD-based FBS, (c) curvelet-based FBS, and (d) TOPS scheme.

III. Examples

In this section, we use both synthetic and field examples to demonstrate the superior performance of our proposed TOPS scheme over traditional FBS scheme regarding seismic reconstruction. All of the following examples are reproducible when MATLAB and Madagascar [19] platforms are both available.

The synthetic data presented here are a combination of several hyperbolic reflectors and several faults. The original data and observed data decimated by randomly removing 50% traces are shown in Fig. 1(a) and (b), respectively. Fig. 2(a), (c), and (e) shows the recovered data using the SVD-based FBS scheme, the curvelet-based FBS scheme, and the proposed double-constrained TOPS scheme, and Fig. 2(b), (d), and (f) displays their corresponding errors compared with the original data shown in Fig. 1(a). The error here means the difference between the reconstructed data and the clean complete data, which is thought to be the exact solution. The eighth crossline sections from Figs. 1(a) and 2(a)–(e) are shown in Fig. 3, from which we can conclude that the proposed TOPS algorithm enjoys a much better reconstruction

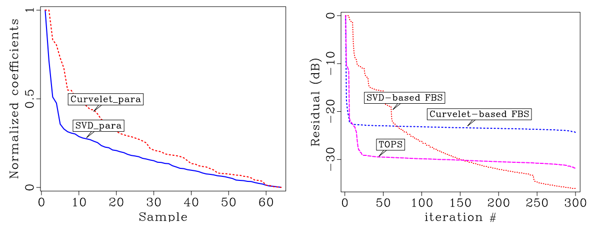

(a) (b)

Fig. 7. (a) Normalized coefficients from SVD and curvelet transform. (b) Convergence diagrams of three algorithms.

TABLE I

MSE AND RUNTIME OF SVD-BASED FBS, CURVELET-BASED FBS, AND TOPS TESTED ON SYNTHETIC AND FIELD DATA

	Models	FBS-svd	FBS-curvelet	TOPS
Synthetic	MSE ($\times 10^{-4}$)	4.005	4.273	3.222
	Runtime (s)	467.4	588.3	723.7
Field	MSE ($\times 10^{-3}$)	2.594	3.064	1.402
	Runtime (s)	39.3	340.8	381.3

performance than the traditional FBS algorithms with single constraint.

The field data example shown in Figs. 4–6 aims to further verify the feasibility and advantage of the TOPS scheme. As shown in Fig. 4(b), we resample the field data by randomly removing 50% traces from the original data shown in Fig. 4(a). Fig. 5(a), (c), and (e) shows the final results using the traditional FBS algorithms and our proposed TOPS algorithm, and their corresponding errors are displayed in Fig. 5(b), (d), and (f), respectively. It is obvious that the proposed approach can obtain an almost perfect recovery [Fig. 5(e)] compared with the original data shown in Fig. 4(a). However, the reconstructed data obtained by SVD-based FBS approach [Fig. 5(a)] suffer from some striped artifacts, which destroy the horizontal consistency of the reflectors. As shown in Fig. 5(c), the seismic data recovered by FBS method by imposing sparsity constraint in curvelet transform domain exhibit better spatial coherency, but remain some notable residual noise compared with the result shown in Fig. 5(e). Fig. 6(a)–(d) shows the eighth crossline slices of Figs. 4 and 5(a), (c), and (e), respectively. From these recovered results in Figs. 5 and 6, we can confirm that the proposed TOPS scheme obtains an obvious improvement in terms of the fidelity and coherency.

In this letter, we thoroughly analyze some important issues about the proposed algorithm, such as parameter selection, convergence property, reconstruction fidelity, and computational complexity. Fig. 7(a) shows normalized coefficients from SVD and curvelet transform, which serves as a reference for selecting an appropriate penalty parameters ω_1 and ω_2 for TOPS (e.g., preserving 50% largest coefficients). Convergence diagrams of three algorithms are shown in Fig. 7(b), which demonstrates the superior convergence property of the proposed TOPS scheme. Besides, to quantify the performance of TOPS algorithm in terms of fidelity and computation, we record the runtime (processor of our laptop is Intel Core i5-4460 CPU @ 3.20 GHz $\times$ 4) and mean square error (MSE) of three algorithms via tests on both synthetic and field data (Table I).

IV. CONCLUSION

We have proposed a novel TOPS scheme for 3-D seismic data reconstruction. In the TOPS framework, we simultaneously consider both SVD-based low-rank constraint and curvelet-domain sparsity constraint. The TOPS can be flexibly used to recover a signal that satisfies simultaneously double convex constraints, and to achieve obviously better data recovery performance than the traditional SVD-based low-rank and curvelet-domain sparsity-based methods following the FBS framework. Both synthetic and field data examples demonstrate the superior performance of the proposed method in obtaining high-fidelity reflection amplitude with less restoration artifacts.

REFERENCES

[1] P. L. Combettes and J.-C. Pesquet, "Proximal splitting methods in signal processing," in *Fixed-Point Algorithms for Inverse Problems in Science and Engineering*, vol. 49. New York, NY, USA: Springer, 2009, pp. 185–212.

[2] Y. Chen, "Iterative deblending with multiple constraints based on shaping regularization," *IEEE Geosci. Remote Sens. Lett.*, vol. 12, no. 11, pp. 2247–2251, Nov. 2015.

[3] G. B. Passty, "Ergodic convergence to a zero of the sum of monotone operators in Hilbert space," *J. Math. Anal. Appl.*, vol. 72, no. 2, pp. 383–390, 1979.

[4] P. L. Lions and B. Mercier, "Splitting algorithms for the sum of two nonlinear operators," *SIAM J. Numer. Anal.*, vol. 16, no. 6, pp. 964–979, 1979.

[5] P. Tseng, *A Modified Forward-Backward Splitting Method for Maximal Monotone Mappings*. Philadelphia, PA, USA: SIAM, 2000.

[6] D. Davis and W. Yin, "A three-operator splitting scheme and its optimization applications," *Mathematics*, vol. 19, no. 3, pp. 407–412, 2015.

[7] P. L. Combettes and V. R. Wajs, "Signal recovery by proximal forward-backward splitting," *Multiscale Model. Simul.*, vol. 4, no. 4, pp. 1168–1200, 2005.

[8] H. Raguet, J. Fadili, and G. Peyr, "A generalized forward-backward splitting," *SIAM J. Imag. Sci.*, vol. 6, no. 3, pp. 1199–1226, 2012.

[9] D. C. Youla and H. Webb, "Image restoration by the method of convex projections: Part 1—Theory," *IEEE Trans. Med. Imag.*, vol. MI-1, no. 2, pp. 81–94, Oct. 1982.

[10] R. Abma and N. Kabir, "3D interpolation of irregular data with a POCS algorithm," *Geophysics*, vol. 71, no. 6, pp. E91–E97, 2006.

[11] I. Daubechies, M. Fornasier, and I. Loris, "Accelerated projected gradient method for linear inverse problems with sparsity constraints," *J. Fourier Anal. Appl.*, vol. 14, no. 5, pp. 764–792, 2008.

[12] S. Gan, S. Wang, Y. Chen, and X. Chen, "Simultaneous-source separation using iterative seislet-frame thresholding," *IEEE Geosci. Remote Sens. Lett.*, vol. 13, no. 2, pp. 197–201, Feb. 2016.

[13] M. D. Sacchi and T. J. Ulrych, "High-resolution velocity gathers and offset space reconstruction," *Geophysics*, vol. 60, no. 4, pp. 1169–1177, 1995.

[14] Y. Chen *et al.*, "Simultaneous denoising and reconstruction of 5-D seismic data via damped rank-reduction method," *Geophys. J. Int.*, vol. 206, no. 3, pp. 1695–1717, 2016.

[15] R. Sternfels, G. Viguier, R. Gondoin, and D. L. Meur, "Multidimensional simultaneous random plus erratic noise attenuation and interpolation for seismic data by joint low-rank and sparse inversion," *Geophysics*, vol. 80, no. 6, pp. WD129–WD141, 2015.

[16] D. Zhang, Y. Zhou, H. Chen, W. Chen, S. Zu, and Y. Chen, "Hybrid rank-sparsity constraint model for simultaneous reconstruction and denoising of 3D seismic data," *Geophysics*, vol. 82, no. 5, pp. 1–111, 2017, doi: 10.1190/geo2016-0557.1.

[17] A. Gholami, "Morphological deconvolution," *Geophysics*, vol. 82, no. 5, pp. V311–V320, 2017.

[18] E. Candès, L. Demanet, D. Donoho, and X. Ying, "Fast discrete curvelet transforms," *Multiscale Model. Simul.*, vol. 5, no. 3, pp. 861–899, Sep. 2006.

[19] S. Fomel, P. Sava, I. Vlad, Y. Liu, and V. Bashkardin, "Madagascar: Open-source software project for multidimensional data analysis and reproducible computational experiments," *J. Open Res. Softw.*, vol. 1, no. 1, p. e8, 2013.